Emerging Contaminants Removal from Wastewater Using Organo-Modified Bentonite Clay

Abdullahi Abdulsalam [a*], Yahya Saleh Ibrahim [b], Nura Alhaji Yaro [a], Olalekan Akeem Olanrewaju [c], Bello Alhassan [d], Dallacoasta Andrea Iyayosa [e] and Kabir Lawal [f]

[a] *School of Health Science, Maryam Abacha American University of Niger, Niger.*
[b] *Centre for Energy and Environmental Strategy Research, Kaduna State University, Nigeria.*
[c] *Chemical Engineering Department, Ahmadu Bello University, Zaria, Nigeria.*
[d] *Entrepreneurship Development Center, Kwara State Polytechnic, Ilorin, Nigeria.*
[e] *Department of Chemical Engineering, Federal University of Technology, Minna, Nigeria.*
[f] *Department of Chemical Engineering, Kaduna Polytechnic, Kaduna, Nigeria.*

Authors' contributions

This work was carried out in collaboration among all authors. All authors contributed to the study conception and design. Material preparation, data collection and analysis were performed by authors AA, YSI, NAY, OAO, BA, DAI and KL. The first draft of the manuscript was written by author AA. Supervision of the manuscript was done by author YSI, review was done by author NAY, formal analysis and investigation was done by author OAO, manuscript resources was provided by author BA, manuscript draft preparation was done by author DAI and manuscript editing was done by author KL. All authors commented on previous versions of the manuscript. All the authors read and approved the final manuscript.

Original Research Article

---

*Corresponding author: Email: abdulsalamabdul81@gmail.com;

ABSTRACT

Organo-modified bentonite clay locally sourced from Bauchi State, Nigeria was prepared and used as an adsorbent for Emerging Contaminants (EC) capture from Kaduna Polytechnic female hostel wastewater. The produced adsorbent was characterized to determine the functional groups, surface area and crystal structure. Surface area for directly modified bentonite clay produced adsorbents and oxalic acid-pretreated bentonite clay adsorbent was found to be 625 m^2/g and 349.2 m^2/g respectively and the morphology of the produced acid-pretreated organo-modified bentonite clay adsorbents has better pore development with a higher amorphous structure. The wastewater compositions were found to contain major ECs identified to be Diclofenac, Triclosan, Methylparaben, a*nd* Bisphenol A, which account for 76.206% of the ECs that are detrimental to human and the environment. The impact of the adsorption factors; contact time, adsorbent dosage, and temperature on uptake behavior were all examined. Effect of adsorbent dosage was established which shows that all ECs removed rise rapidly from 0.5 – 1.0 g adsorbent dosage and then slowly reach a maximum of 98.65% Triclosan, 95.83% Diclofenac, 91.49% BPA, and 62.16% Methyl-Paraben removal as adsorbent dosage increases to 2g. On the other hand, as the adsorbent dosage increases to 3g, the removal rate of all ECs was observed to drop slightly and then attain maximum removal as the dosage rises to 4g. In contrast, a rise in adsorbent dosage of 2.5g gives a sudden drop in removal of Triclosane to 92.41% and Methyl-Paraben to 53.01% as well as a sharp drop in Methyl-Paraben to 33.33% and slightly drop in the removal of all other ECs. Langmuir and Freundlich isotherms models were fitted to the adsorption data and Freundlich showed best fit indicating chemisorption. The adsorption of triclosan, diclofenac, bisphenol A, and methylparaben followed pseudo second-order kinetic model.

1. INTRODUCTION

The generated domestic and industrial wastewater is frequently dumped directly into the receiving medium, such as the ocean, river, or soil, without first undergoing pre-treatment. Uncontrolled wastewater discharge can pollute the environment and pose several health risks [1]. Most of the time, domestic and industrial wastewater is contaminated with toxic and poisonous chemicals, and other pollutants that hurt the environment. Recently, it has been discovered that domestic wastewater contains organic contaminants of emerging concern that are derived from infrastructure and human and household products and are widely dispersed throughout the environmental matrices, whereas industrial wastewater refers to a variety of wastewater that is produced because of industrial activities [2,3].

Water quality, pollution, and scarcity are currently the three most significant environmental problems. Environmental illnesses and contamination difficulties have not been the only problems brought about by technological advancement. The discharge of home, industrial, and municipal wastes—including colored effluents, which are among the worst pollutants—is the primary cause of aquatic contamination. Water pollution is frequently caused by the presence of organic and/or inorganic molecules, including dyes. Specifically, colored pigments should not be present in water or effluents generally because they are harmful to human health, mutagenesis, and organism life. [4]. Due to the advancement of medical services and products like contaminated wastes, including natural and synthetic dangerous substances, etc., wastewater effluent from hospitals has increased over the past few decades. This presents adverse effects to all living things [5, 6]. Many species of fish, birds, and marine animals have been adversely affected, thereby affecting public health [7, 6]. Some of these poisonous substances have caused serious environmental dangers and the deaths of sea birds and other aquatic animals.

The total removal and elimination of a variety of contaminants that are causing developing environmental concerns in different biological and environmental wastewater are inefficient by traditional treatment approaches. The issue of removing pollutants from water is a significant one that is getting worse due to the expansion of industrial activities and the emergence of toxins in home wastewater around the world [8, 6]. This

makes wastewater treatment for EC- and industrial pollutant contamination necessary. Even with modern technologies, some of these contaminants may generally be removed from wastewater using traditional techniques like physical or chemical approaches, but these techniques are frequently pricy and challenging to maintain [5].

Because of their high efficiency, ease of handling, and economic viability, physical methods, such as sorption, are particularly regarded as a straightforward and suitable strategy for pollutant removal in polluted wastewater [9,3]. Membrane processes and biological materials are among other technologies that was employed to trap pollutants from contaminated wastewater. These methodological approaches are only employed in unique situations of wastewater treatment because they are extremely expensive, economically undesirable, or technically challenging. The adsorption of these ECs from wastewater by employing natural material was a relatively new green method for the treatment of ECs in wastewater. Diverse physical, chemical, and biological treatment approaches, including ozone treatments, coagulation, reverse osmosis, ionization exchange, photocatalysis, oxidation, and adsorption, are employed to eliminate colors from water and wastewater [10-17].

The use of natural materials in the adsorption process has proven to be a highly effective technique for treating contaminated wastewater since it has several benefits including affordability, availability, profitability, simplicity of use, and efficiency [18]. Therefore, the use of natural materials in adsorbent preparations is encouraged by their moderately lower cost, their ability to be produced locally in many nations, including the Republic of Niger and Nigeria, as well as their efficiency in removing a variety of contaminants from wastewater.

For wastewater treatment, a variety of materials have been used as adsorbents, including activated carbon from industrial waste, agricultural waste, clay materials, and hybrid diatomite/carbon composites [19, 20, 5, 21, 18 22, 3]. It is necessary to develop and produce organo-modified adsorbents from low-cost raw materials like activated carbon from agricultural waste and clay, which is easily accessible in abundance in nations like the Niger Republic and Nigeria for ECs removal in wastewater because applying these materials as adsorbent is limited

due to relatively low removal efficiency. Therefore, it is necessary to find environmentally beneficial and reasonably priced methods for removing contaminants from the environment. Adsorption technology is one of the most effective techniques for eliminating both organic and inorganic contaminants from wastewater and water. Because it is easy to use, inexpensive, highly efficient, and doesn't create any undesirable byproducts, adsorption is a viable method for treating wastewater. The adsorption approach also has the benefit of being simple to develop and use, as it can remove a wide range of contaminants from aqueous solutions. Conversely, because adsorption requires a strong separation between the adsorbent and the pollutant, it has drawbacks such as low selectivity and harmful waste products. A variety of materials, such as metal oxides, polymers, carbon nanotubes, activated carbon, zeolite, clay, agricultural solid waste, and graphene, can be utilized as dye absorbents [23-31].

Activated carbon and clay materials like natural clay, bentonite, and kaolin clay have been used in several studies to treat wastewater effluents because they are effective alternatives to traditional adsorbents [19, 18, 32, 3]. Need to research the organic modification of clay material for adsorption and removal of ECs from wastewater was driven by the abundance of bentonite clay deposit in Nigeria and some other countries, which is of great significance in adsorption of pollutants from wastewater.

2. METHODOLOGY

This section describes the experimental methods used to produce an organo-modified bentonite clay adsorbent and characterizes the resulting adsorbents and effluent for ECs. Additionally, this chapter presents the experimental techniques used to examine the produced adsorbents' adsorption effectiveness as well as their adsorption isotherm models and adsorption kinetics for ECs removal from wastewater.

2.1 Sample Preparation

2.1.1 Bentonite clay sample preparation

Bentonite clay was acquired at Bauchi L.G.A., Bauchi State. Stones and other non-clay particles were manually removed from the samples, and the remaining larger non-clay

fractions were crushed and sieved using a mesh sieve. Bentonite clay samples that have been sieved would be dissolved in distilled water that has been acidified with HCl and continually swirled with a stirrer to create two layers: a layer of larger particles that can settle and a layer of colloidal suspension that contains the bentonite clay. The colloidal layer would then be recovered after the suspended layer had been carefully decanted. To get rid of any remaining impurities, the supernatant must be decanted, and the bentonite clay thoroughly rinsed with distilled water. The impurity-free bentonite clay was recovered and oven-dried at 100 °C to produce dried bentonite clay samples. To create an organo-modified bentonite clay adsorbent, the prepared bentonite clay was mashed, sieved to a mesh size of 350 m, and then maintained in a closed container.

2.1.2 Organo-modified bentonite clay

According to the method described by [33] the organo-modified bentonite clay was made using a cation exchange reaction procedure. Bentonite clay that had been manufactured was agitated (4% w/w) for 30 minutes while being mixed with distilled water, and it was then left to settle for a day. The suspension was combined with CTMABr, and the mixture was vigorously agitated for 20 minutes before being allowed to settle for a day. Filtered out, the organo-modified bentonite clay was then dried at 60.5 °C to attain constant weight. The produced organo-modified bentonite clay was then grounded and sieved to a thickness of around 200 microns and stored in

a sample container followed by characterization and adsorption research.

2.2 Adsorbent Characterization

Various characterization techniques were used to examine the structural, morphological, functional, and optical characteristics of as-synthesized nanomaterials. According to the characterization techniques used by [34,35] that The produced modified bentonite clay was characterized using FTIR, XRD, and BET analyzers to establish the functional groups using the Shimadzu FTIR-8400S analyzer, determination of the crystal structure obtained using XPERT-PRO X-ray diffractometer and determination of surface area, volume of pores pore size were performed using Micromeritis Tristar 3000 surface area analyzer device.

2.3 Wastewater Sampling and Collection

The main considerations for the wastewater sampling strategy in this study are for diagnostic evaluation and targeting of pollutants in the wastewater stream. The sampling locations selected in this study for the wastewater collection are the Kaduna Polytechnic female hostel wastewater source and drainages where the wastewater from different sources was well mixed as the representative collection site. The Grab sampling technique was utilized to collect the wastewater samples over a period that does not more than 15 minutes. Wastewater was collected using the grab sampling technique at roughly 9 AM. 5-liter samples of wastewater were taken from the sampling location.

Fig. 1. Some of the photos taken during the experimental research

2.4 Wastewater Characterization

The wastewater used in this study was characterized to determine its constituent and ECs present in the wastewater. The wastewater collected was characterized to determine qualitative and quantitative ECs present in the wastewater using an HPLC-UV spectrometry analyzer. The NIST library was used to identify all the chemicals. Operating conditions for the mass spectrometer included a range of 40 to 1000 m/z at an interface temperature of 240 ℃, and an ion source temperature of 200 ℃. Additionally, the concentration of the several detected ECs from GCMS analysis was determined using a UV Spectrophotometer.

2.5 Batch Adsorption Study

Batch process was used to obtain equilibrium data. 1g of adsorbent (organo-modified activated carbon) was contacted with 20 mL of the pretreated wastewater in an adsorption column with a known initial concentration at a pH of 6 – 7. Experiment proceeds to attain the equilibrium condition at room temperature. A separation between liquid and solid phases occurred at the designated equilibrium time. Using a UV-visible spectrophotometer, samples of supernatant were obtained as concentration of un-adsorbed ECs was found. Equilibrium adsorption capacities (q_e) of the organo-modified adsorbent samples were calculated using the equation 1.

$$q_e = \frac{(C_o - C_f)\, x\, V}{M} \tag{1}$$

where Co and Ce are the initial and equilibrium concentrations of ECs in the solution (in mg/L), respectively, and qe is the adsorption capacity of ECs in an aqueous solution (in mg/g). M is the mass of the adsorbent (g), and V is the volume of the aqueous solution (ml).

The ECs adsorption efficiency which is the ratio of the difference between initial and equilibrium concentration divided by initial concentration expressed in percentage would be determined using equation 2.

$$\text{Removal Efficiency} = \frac{C_o - C_f}{C_o}\, x\, 100 \tag{2}$$

where, C_o = Initial concentration and C_f = final concentration after

3. RESULTS AND DISCUSSION

3.1 Characterization of Wastewater

The wastewater used in this study was characterized to determine its constituent and ECs present in the wastewater. The wastewater collected was characterized using HPLC-UV spectrometry instrument to determine the ECs present in the wastewater and quantity of each ECs in the wastewater.

Table 1 shows the major identified ECs from the analyzed wastewater. Triclosan accounted for 24.955% of the in the wastewater followed by Diclofenac, Bisphenol A and Methylparaben which account for 21.772%, 16.805% and 12.674% of the identified ECs respectively. Also 6.464% Syringoside, 1.778% Adenine and 1.428% Calycosin-7-O-β-D-Glucopyranoside were identified from the HPLC analysis of the wastewater. The obtained result shows that Diclofenac, Triclosan, Methyl paraben and Bisphenol A are the major ECs in the wastewater which account for 76.206% of the total contaminants in the water. The high concentration of Triclosan detected from the analysis could be attributed to rise in the used of personal care products mostly by the female gender which are rinse and washed off into drainage and then to surface water. This corroborated by [36, 32] assertions that major source of Triclosan in wastewater from personal care products such as musk fragrances and antimicrobials.

Table 1. Identified ECs in the wastewater from the HPLC chromatogram

Max. Wavelength (nm)	Retention Time (min)	Area (%)	Identified ECs
276	7.3073	24.955	Diclofenac
352	14.3372	21.772	Triclosan
254	1.46	16.805	Methylparaben
229.5	11.2566	12.674	Bisphenol A
267	12.5779	6.464	Syringoside
260	3.581	1.778	Adenine
258	19.632	1.428	Calycosin-7-O-β-D-Glucopyranoside

Also, Table 1 shows that Diclofenac has the highest concentration in the wastewater which is an anti-inflammatory drug which could result to compromising health of stream biofilms organisms on exposure [37, 3]. Similarly, Methylparaben (16.805%) and Bisphenol A (12.674%) reported to be of major ECs of concern and have gained much attention in recent years because of their demonstrated ability to cause endocrine disruption [38, 39, 32, 3]. Hence, the major ECs identified using HPLC from wastewater are mainly Diclofenac, Triclosan, Methylparaben and Bisphenol A which portends demonstrated ability to be detrimental to human health and environments. To this end, the adsorption and kinetics studies will focus on the first four ECs (Diclofenac, Triclosan, Methylparaben and Bisphenol A) with the highest concentration which account for 76.206% of the ECs in the wastewater.

3.2 Adsorbent Characterization

3.2.1. X-Ray Diffraction (XRD) analysis

Crystal structure of produced organo-modified bentonite clay adsorbents was analyzed.

Figs. 3 and 4 highlighted the XRD pattern of produced organo-modified bentonite clay adsorbents. Fig. 3 shows the XRD pattern of the produced oxalic acid pretreated organo-modified bentonite clay before adsorption (DMB). It was observed that diffraction peak at 2θ angle of 26.67° was mainly diffraction peak of quartz and shows that the DMB adsorbent is mainly crystalline silica of quartz [40]. The 2θ angle of 5.34°, 34.14° and 60.06° are typical of the presence of hydrobiotite in the produced organo-modified bentonite adsorbent (DMB) and 10.2% urea presence in the crystal structure, which is an indication that the Cetyltrimethylammonium bromide (CTMABr) cations were intercalated into the bentonite clay structure [41, 21, 18]. From the XRD analysis shown in Fig. 3, the basal spacing of the produced DMB adsorbent at 2θ angle of 26.67° was 3.343 Å, indicating the 1 0 1 plane of quartz while the peak at 2θ angle of 20.89° and 50.04° were also typical of quartz.

The basal spacing of the produced DMB at 2θ angle of 20.89° was 3.189 Å, indicating the 0 0 2 planes of albite [42]. The diffractograms shown in Fig. 3 indicates that the crystal structure comprises mainly of quarts and hydrobiotite with the highest intensity of 1584 count comprising of 52.3% quartz, 17.4% graphite, 20.10% hydrobiotite and 10.20% urea in the produced oxalic acid DMB adsorbent. Furthermore, the high basal spacing in the presence of the quaternary salt (CTMABr) is known to facilitate the intercalation of the DMB adsorbent.
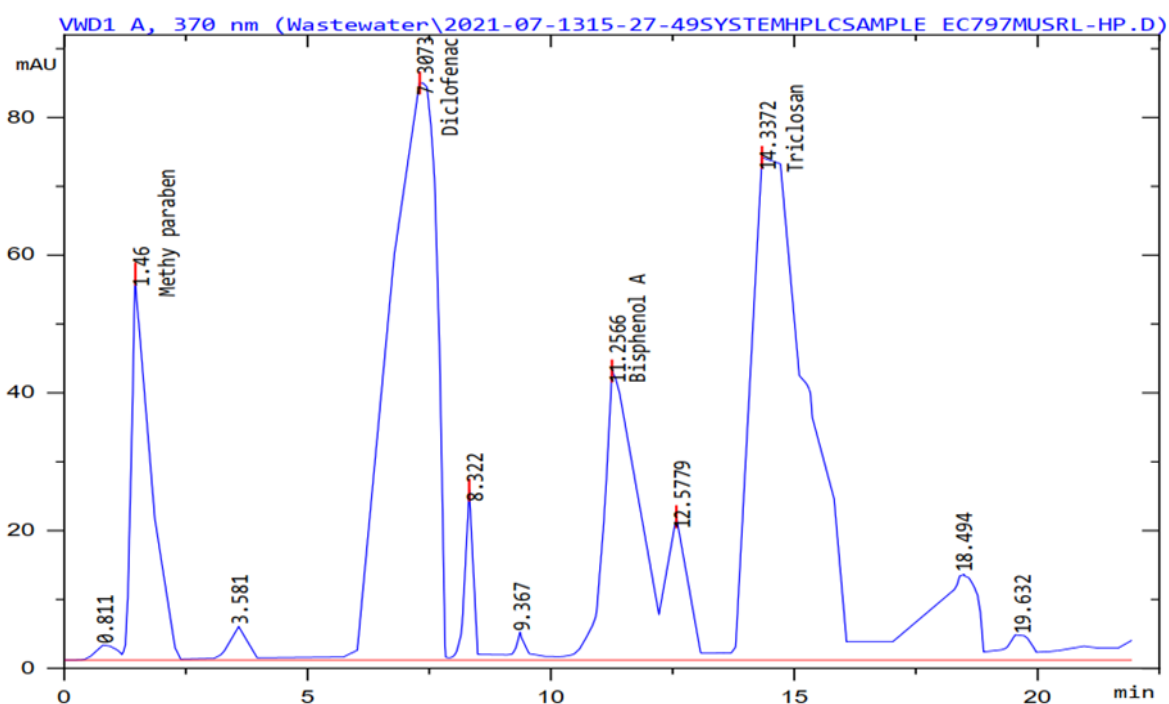

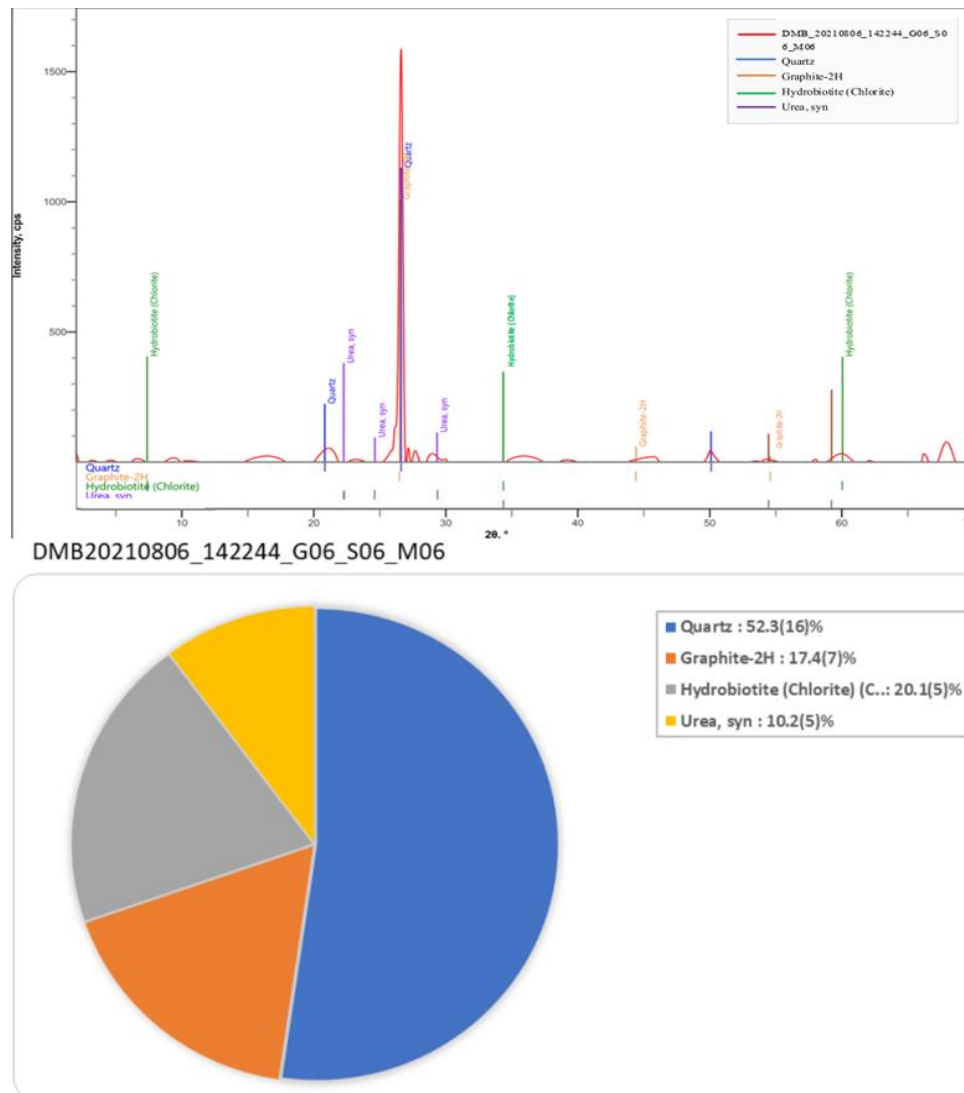**Fig. 2. HPLC Fingerprint Analysis of Wastewater**

Fig. 3. XRD pattern of modified bentonite (DMB) adsorbent before adsorption

The produced oxalic acid pretreated modified bentonite clay adsorbent was also characterized after usage for adsorption of ECs in the wastewater. The oxalic acid pretreated modified bentonite clay adsorbent with the highest ECs removal during adsorption, tag as APMB, was also characterized to the if the ECs adsorption have effect on the crystal structure of the adsorbent. Fig. 4 present the XRD pattern of oxalic acid pretreated modified bentonite adsorbent after adsorption (APMB).

Fig. 4 shows similar diffraction peak at 2θ angle of 26.67° of quartz as well as 2θ angle of 34.14° and 60.06° of hydrobiotite in the crystal structure of the produced organo-modified bentonite adsorbent after adsorption. This peak corresponds to (101) planes of crystallographic planes which was assigned to quartz of

montmorillonite phase [42]. In like manner, the hydrobiotite presence with monoclinic structure is similar to that before ECs adsorption (Fig. 4). Peaks found correlated with basal spacing that was reported in literatures for montmorillonite and monoclinic silicate phase [43, 44, 45]. The XRD analysis shows that APMB adsorbent made up of mainly of montmorillonite and monoclinic silicate phase. However, it was seen that the composition of the crystal system after ECs adsorption changes and comprises of 43% quartz, 14.3% graphite, 16.5% hydrobiotite, 8.4% urea and 17.8% garnet (nesosilicate). This indicates that, adsorption of ECs by the produced oxalic acid organo-modified bentonite adsorbent affects the crystal structure of the APMB adsorbent due to the presence of garnet silicate phase (octahedral and tetrahedral structure) presence after adsorption [46].

127

The generated results depicted that the level of crystallinity reflected for the DMB adsorbent (before adsorption) is relatively low with corresponding high rate of amorphous silica phase, which gives very good capacity for the modified adsorbent. [41, 47]. This confirms high ECs removal by the produced oxalic acid pretreated organo-modified bentonite clay adsorbent. Hence, the crystal structure of the produced DMB adsorbent indicates high adsorption capacity of the adsorbents.

3.2.2 Fourier Transform Infra-Red (FT-IR) analysis

The FTIR, which is a measure of the organic and inorganic functional group present in a material was also determined. The FTIR spectrum of the produced acid pretreated modified bentonite adsorbent (DMB) and (APMB) adsorption was presented in Fig. 5 (a) and (b). FTIR spectra of DMB as shown in Fig. 5 (a), shows the fingerprint band for bending vibration of Si–O–Si and Si–O–Al between 689.6 – 998.9 cm^{-1}, indicating the presence of silicate montmorillonite as well as C–Br stretch. Band at 749.2 cm^{-1} and 779.7 cm^{-1} are attributed to Si-O vibration and Si–O stretching vibration respectively which are made up of quartz silicate of montmorillonite phase in the bentonite [48, 44]. Likewise, band at 909.5 cm^{-1}, 998.9 cm^{-1} are associated with Si–O–Al stretching mode for montmorillonite and, Si-O stretching and out of plane Si–O–Si stretching mode of octahedral sheet montmorillonite (bentonite) respectively [44].
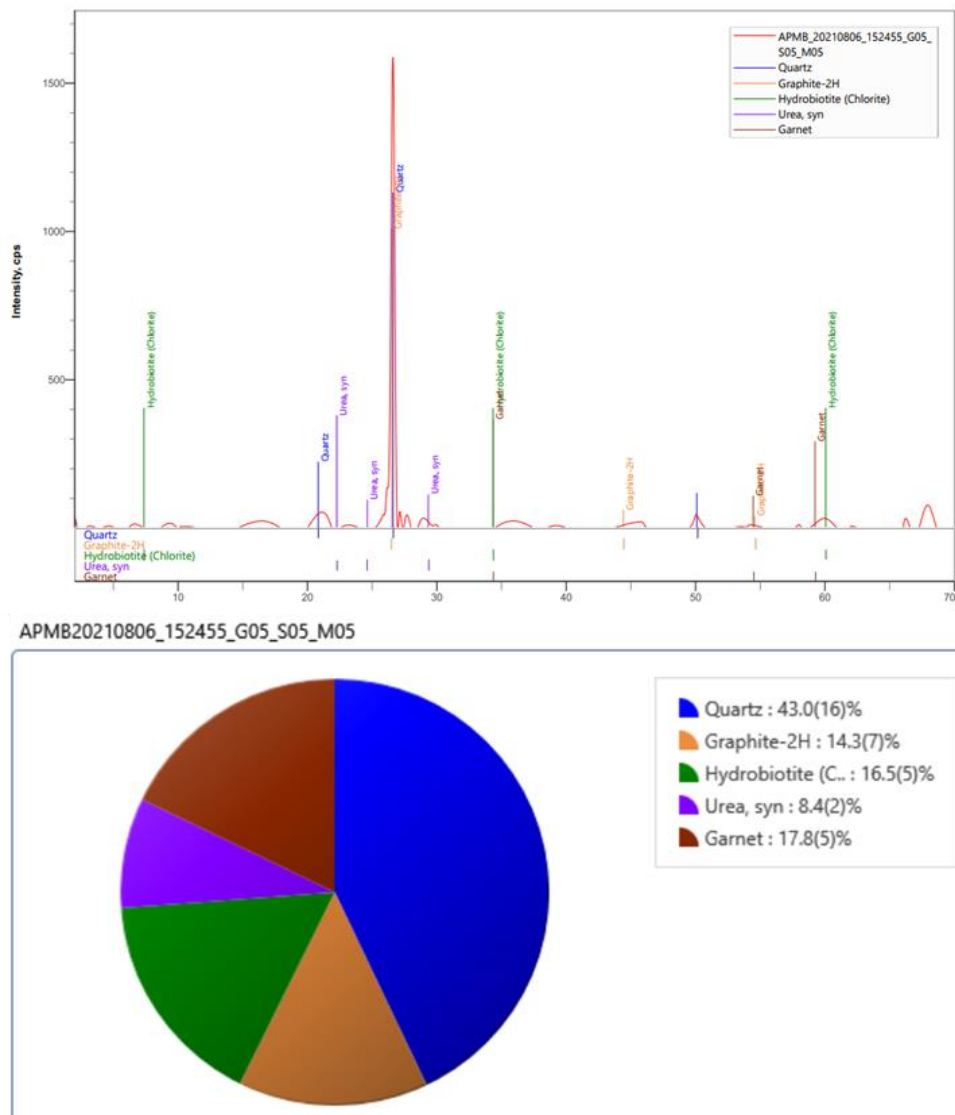

Fig. 4. XRD pattern of acid pretreated modified bentonite (APMB) adsorbent after adsorption

From Fig. 5 (a), the band at 1468.6 cm^{-1} is due to C–H bend vibration, and band at 1640 cm^{-1} is due to C=C stretching mode as well as weak N-H bend which are attributed to the presence of quaternary salt [49]. The band at 2851.4 cm^{-1} 2922.2 cm^{-1} is also attributed to strong C-H stretch of alkane and alkyls group which are associated with the organic quaternary salt used for modification. The band at 3623–3697.5 cm-1 is related to –OH vibration mode and –OH stretching mode for water that has been absorbed between the layers of montmorillonite. This fits with what the literature says about the OH band for water [47, 50, 51, 44]. Furthermore, band at 3697.7 cm^{-1} is associated with O-H stretching vibrations in Si-OH and Al-OH groups of tetrahedral, octahedral sheets of montmorillonite and hydrobiotite phase of acid modified bentonite clay adsorbent before adsorption of ECs. [50] found for Si-OH and Al-OH groups of tetrahedral sheets of montmorillonite silicate. XRD research showed that montmorillonite and hydrobiotite were present in DMB adsorbent, which backs this up.

Fig. 5 (b) also, presents the FTIR analysis of the oxalic acid pretreated organo-modified bentonite clay adsorbent (APMB). It was observed that there was a change in the structural orderliness in the number and sharpness of peak with the oxalic acid APMB adsorbent shown in Fig. 5 (b) after ECs adsorption compared to that of DMB, before ECs adsorption (Fig. 5 (a)). It was reported by [52, 42] that major infrared characteristic peaks of quartz and microcline occur between 400 – 1300 cm^{-1}. In this range, there were similar bands in the range of 689.6 – 998.9 cm^{-1}, representing fingerprint band for Si–O–Si and Si–O–Al bending vibration like those observed in the DMB adsorbent. These peaks indicated the presence of Si-O-Si bending vibration and coupling between the O–Si–O deformation stretching [53]. The band at 1140.6
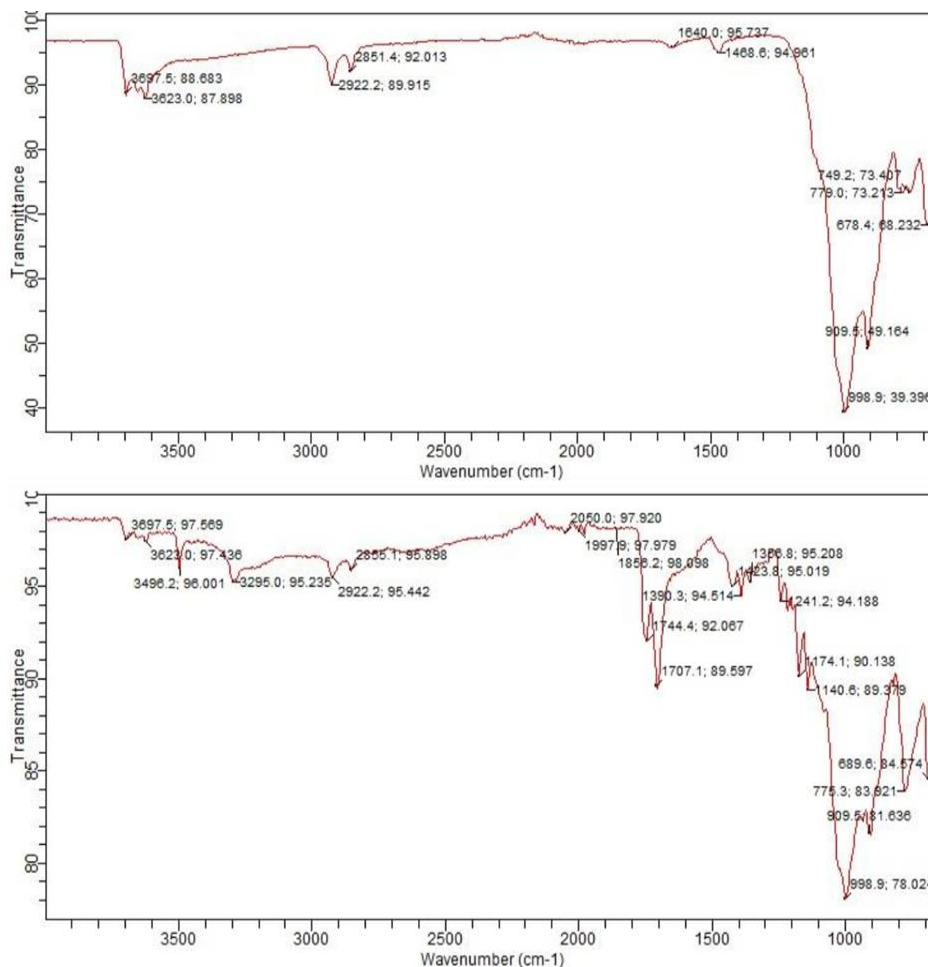

Fig. 5. FTIR analysis of acid pretreated modified bentonite adsorbent (a) before (DMB) and (b) after (APMB) adsorption

and 1174.1 cm^{-1} is associated with C–O stretch and medium C–N stretching which was attributed to alkyl aryl ether and amine group respectively while the band at 1241.2 – 1390.3 cm^{-1} is associated with medium C–H bending of aldehyde group. Furthermore, from Fig. 4.6(b), 1707.1 – 1744.4 cm^{-1} is associated with C=O stretching of strong monomer of carboxylic acid group and C–N of amine group whereas, the absorption band at 1858.2 – 2050 cm^{-1} is associated with weak C–H bending of aromatic functional group [42].

The bands between 2800 – 3000 cm^{-1}, particularly 2855.1 cm^{-1} and 2922.2 cm^{-1} for acid pretreated modified bentonite adsorbent (APMB), (Fig. 5b) and that between 2851.4 cm^{-1} and 2922 cm^{-1} for acid pretreated modified bentonite adsorbent (DMB) (Fig. 5a), indicates C-H stretch for amine and methyl C=O for acid respectively. The bands located at 3295 – 3697 cm^{-1} for both APMB and DMB adsorbent are the typical indications of inner-surface hydroxyls (O-H) group and the one at 3623 cm^{-1} was linked to stretching frequency of internal hydroxyl groups and N-H amine group. The FTIR bands of both APMB and DMB adsorbents further confirm the intercalation of alkylammonium in the interlayer of galleries of the produced bentonite clay

adsorbent [54, 42]. Fig. 5 (a) and (b), shows the similarity in the identify functional group, however, Fig. 5 (b) show the presence of more hydrocarbon functional group, further confirming the presence of organic compound ECs after usage for adsorption of ECs.

3.2.3 Brunauer–Emmett–Teller (BET) analysis

Before and after being used to treat wastewater, the microporosity of the created adsorbents is a key factor in how well they work. To do this, the surface area, pore volume, and pore size of the oxalic acid-treated bentonite clay before and after use are key factors for successful pollutant removal by adsorbent. Using the Quantachrome device, the BET method was employed to measure total surface area and volume of pores of adsorbents. The BJH, DH, and DFT methods were used to measure total adsorption surface area and volume of the micro and macropores. The t-method was employed to measure the external surface area, and the DR method was utilized to measure the micropore area of the created adsorbents. [55]. IUPAC divides porosity into three groups based on the size of the pores: micropores of 2 nm width, mesopores width of 2–50 nm and macropores width greater than 50 nm. BET surface area measurement of the adsorbent is shown in Table 4.

Table 2. BET surface area analysis

Surface Area	DMB	APMB
	Before (m²/g)	After (m²/g)
Single Point BET	367.70	245.40
Multi Point BET	625.00	349.20
Langmuir Surface Area	8617.00	5163.00
BJH Method Cumulative Adsorption Surface Area	605.80	289.50
DH Method Cumulative Adsorption surface Area	566.90	344.20
t-Method External Surface Area	523.00	371.10
DR Method Micropore Area	596.90	329.30
DFT Cumulative Surface Area	157.40	58.14
Pore Volume	**cm³/g**	**cm³/g**
BJH Method Cumulative Adsorption Pore Volume	0.3680	0.1640
DH Method Cumulative Adsorption Pore Volume	0.2586	0.2187
DR Method Micropore Volume	0.2062	0.1040
HK Method Micropore Volume	0.0669	0.0522
SF Method Micropore Volume	0.0121	0.0259
DFT Method Cumulative Pore Volume	0.1431	0.0680
Pore Size	**nm**	**nm**
BJH Method Cumulative Adsorption Pore Diameter (Mode Dv(d))	2.311	2.132
DH Method Cumulative Adsorption Pore Diameter (Mode Dv(d))	2.542	2.521
DR Method Micropore Pore Width	6.538	5.749
DA Method Pore Diameter (Mode)	2.770	2.680
HK Method Pore Diameter (Mode)	1.551	1.986
SF Method Pore Diameter (Mode)	3.788	2.991
DFT Pore Diameter (Mode)	2.574	2.711

Table 2 present surface area, pore volume and pore size of produced oxalic acid pretreated organo-modified adsorbent before and after usage for adsorption of ECs from wastewater. The surface areas for the produced bentonite adsorbents were found to have high pore surface area. This further corroborate the finding from the XRD analysis which shows produced bentonite adsorbents have high amorphous content. The higher specific surface area of the produced bentonite adsorbent portends high adsorption capacity of the bentonite adsorbent. After the produced modified bentonite adsorbents have been used for ECs adsorption from wastewater, the specific surface area of the adsorbents was found to reduced, indicating that foreign materials (ECs) have been adsorbed into the pores of the adsorbents. Equally, the pore volume of the adsorbents can be regarded as other important parameter. From Table 2, substantiating the adsorption surface area of the adsorbents and micropore volume of the adsorbents. Pore volume of produced bentonite adsorbent is high for all methods except for DH and DFT method. This further shows that acid pretreated organo-modified bentonite adsorbent possesses higher adsorption capacity compared to DMB adsorbent. This could be because acid pretreatment of the adsorbent precursor before modification with alkylammonium salt led to a high growth of the pores in the adsorbent.

3.3 Effect of Contact Time

Effect of contact time on adsorption capacity of formed adsorbents (oxalic acid-treated sample and untreated sample) was studied in an adsorption study. The ECs adsorption study was limited to the first four ECs identified in the wastewater (Table 5) with highest concentration. Fig. 6 (a) depicts the effect of contact time on the adsorption of ECs (Triclosane, Diclofenac, BPA and Methyl-paraben) using oxalic acid pretreated organo-modified bentonite adsorbent from 0 – 60 minutes. The adsorption profile shows that there was almost linear and rapid uptake of Triclosane, Diclofenac and BPA to over 90% removal each in first 40 min of adsorption time while the uptake of Methyl-paraben reach 52.32% removal after 40 min. The fast initial uptake of the ECs can be link to presence of many adsorption sites available on adsorbents for the retention of organic molecules [41, 18, 56, 22]. However, as contact time increases beyond 40 min, the rate of removal of Triclosane, Diclofenac and BPA remain almost constant at a maximum removal of 98.55%, 95.69% and 90.07% respectively while

the maximum removal of Methyl-paraben beyond 40 min is 52.73%. This is because as the ECs are adsorbed onto the active sites of the adsorbent particles, the number of possible active sites goes down. As the adsorption rate goes down, the slope of the graph flattens [57].

Also, synonymous trend was noticed with the utilization of direct organo-modified bentonite adsorbent shown in Fig. 6 (b) for the adsorption of ECs (Triclosane, Diclofenac, BPA and Methyl-paraben) from wastewater. Rapid and fluctuating rise in the removal of ECs was observed from 0 – 40 min for all ECs while the removal rate remains almost the same beyond 40 min to a maximum removal of 87.43%, 82.50%, 82.27% and 57.51% for Triclosane, Diclofenac, BPA and Methyl-paraben respectively. This infers that continuous adsorption beyond 40 min do not portend any significant impact on the percentage removal of ECs by both adsorbents.

Conversely, it was observed that oxalic acid pretreated modified bentonite adsorbent (Fig. 6a) give higher removal rate of 98.55% Triclosane, 95.69% Diclofenac, 90.07% BPA and 52.73% Methyl-paraben compared to using direct modified bentonite adsorbent (Fig. 6b) which give a slightly lower removal rate of 87.43% Triclosane, 82.50% Diclofenac and 82.27% BPA, except for Methyl-paraben which give higher removal of 57.51%. This infers that oxalic acid pretreatment of the bentonite clay material before modification enhances the removal of Triclosane, Diclofenac and BPA while non-treatment with oxalic acid favors the removal of Methyl-paraben.

3.4 Effect of Adsorbent Dosage

Adsorption study was done to evaluate effect of adsorbent dosage on the ECs removal capacity of the produced organo-modified bentonite clay adsorbents. Fig. 7 presents effect of adsorbent dosage (0.5 – 4.0 g) on the adsorption of the identified ECs from wastewater using oxalic acid pretreated organo-modified bentonite (Fig. 7a) and direct organo-modified bentonite (Fig. 7b) adsorbent. Fig. 7a shows that the amount of all ECs removed rises rapidly from 0.5 – 1.0 g adsorbent dosage and then slowly to reach a maximum of 100% Triclosane, 99.86% Diclofenac, 92.91% BPA and 69.26% Methyl-Paraben removal as adsorbent dosage increases to 2 g. On the other hand, as adsorbent dosage increases to 3g, the removal rate of all ECs was observed to drop slightly and then attain

maximum removal as dosage rises to 4g. Equally, same trend was observed with the use of direct organo-modified bentonite adsorbent shown in Fig. 7b. Fig. 7b shows the amount of all ECs removed rises rapidly from 0.5 – 1.0 g adsorbent dosage and then slowly to reach a maximum of 98.65% Triclosane, 95.83% Diclofenac, 91.49% BPA and 62.16% Methyl-Paraben removal as adsorbent dosage rises to 2g. In contrast, rise in adsorbent dosage 2.5g led to sharp drop in the removal of Triclosane to 92.41% and Methyl-Paraben to 53.01% as well as a sharp drop in Methyl-Paraben to 33.33% and slightly drop in the removal of all other ECs.

The rapid rise in percentage removal of Triclosane, Diclofenac, BPA and Methyl-Paraben as adsorbent dosage increases because of the high number of adsorption sites available per unit mass of adsorbents [58, 59, 33]. The consistent percentage removal observed within the range of 2-4 g of adsorbent dosage can be attributed to the following factors: at low adsorbent dosage, the adsorption sites are dispersed in the solution, allowing for effective interaction with the environmentally concerning substances (ECs) present in the polluted water. Conversely, at high adsorbent dosage, there is a possibility of adsorbent aggregation in the polluted water, leading to negligible removal of ECs [58, 45].
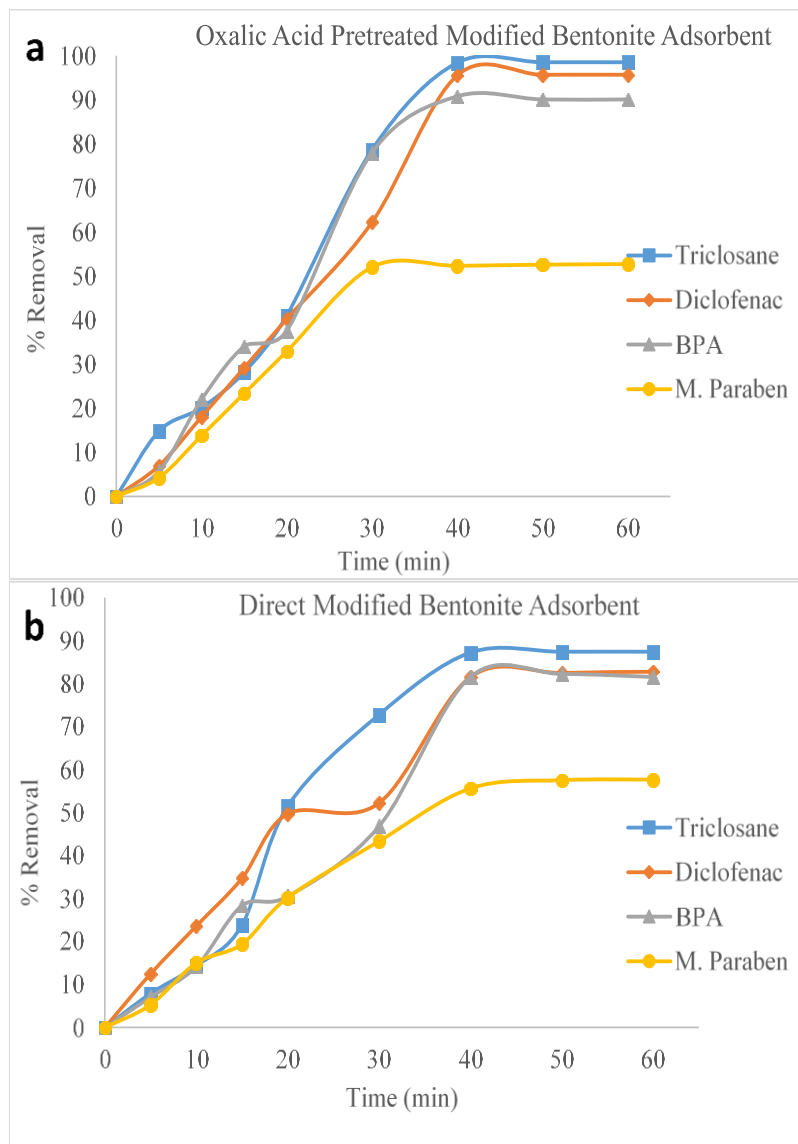

Fig. 6. Effect of contact time on ECs removal (a) Oxalic acid pretreated and (b) Direct organo-modified bentonite adsorbent

Also, the effect of adsorbent dosage shows that oxalic acid pretreated modified bentonite adsorbent gives higher ECs removal from the wastewater compared to direct modified bentonite adsorbent.

3.5 Effect of Adsorption Temperature

Effect of temperature on the adsorption of ECs from wastewater using the produced adsorbents were studied at varying temperatures (25 – 60 °C). Fig. 8 presents the effect of temperature on adsorption of identified ECs from wastewater using oxalic acid pretreated organo-modified bentonite (Fig. 8a) and direct organo-modified bentonite (Fig. 8b) adsorbent. Fig. 8a shows that the amount of all ECs removed rises rapidly to reach a maximum percentage removal of 87.53% Triclosane, 88.47% Diclofenac, 87.94% BPA and

70.63% Methyl-Paraben as temperature rise from 25 – 35 °C and further rise in temperature to 60 °C shows a gradual decline in percentage removal of Triclosane, Diclofenac, BPA and Methyl-Paraben to 75.06%, 66.67%, 76.60% and 62.16% respectively. In the same manner, Fig. 8b shows a maximum rise of 86.49%, 84.72%, 82.27% and 62.16% removal of Triclosane, Diclofenac, BPA and Methyl-Paraben respectively as temperature rise from 25 – 35 °C for direct modified bentonite adsorbent with a continuous decline in percentage removal to reach 75.06% Triclosan, 81.67% Diclofenac, 72.34% BPA and 33.33% Methyl-Paraben when temperature rises to 60 °C. The adsorption profile in Fig. 8 (a) and (b) shows implies that the adsorption of ECs into both bentonite adsorbent decreases as temperature increases.
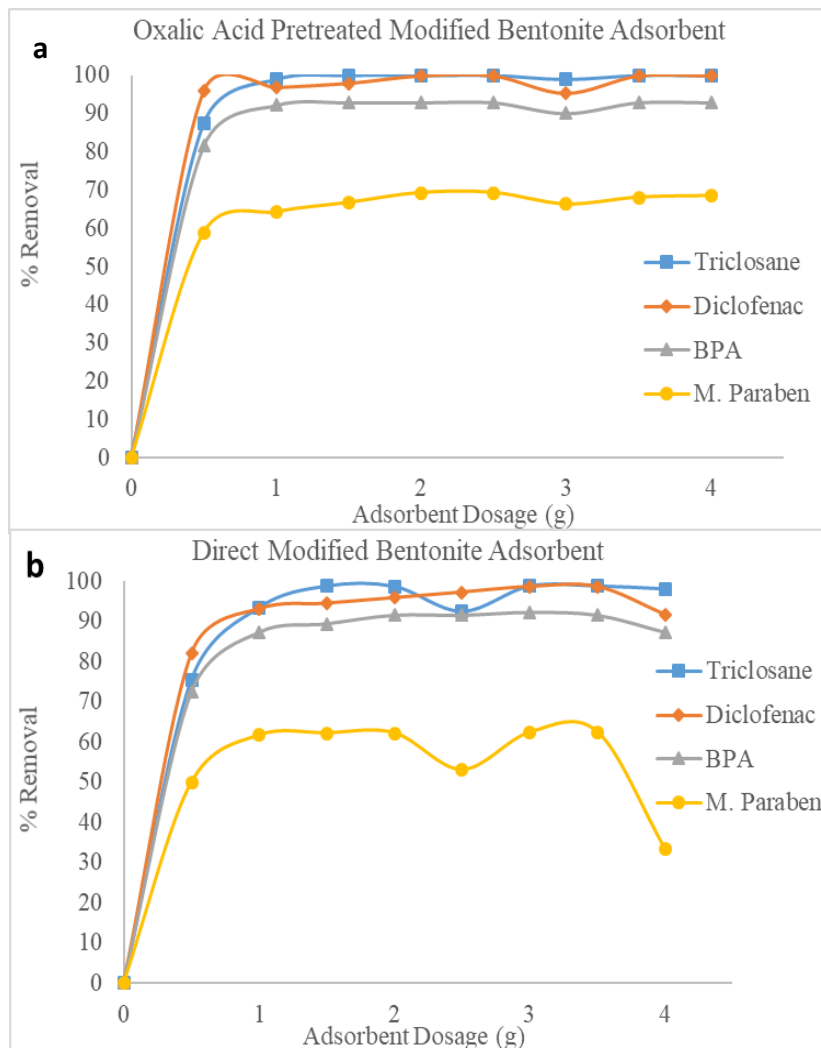

Fig. 7. Effect of adsorbent dosage on ECs removal (a) Oxalic acid pretreated and (b) Direct organo-modified bentonite adsorbent
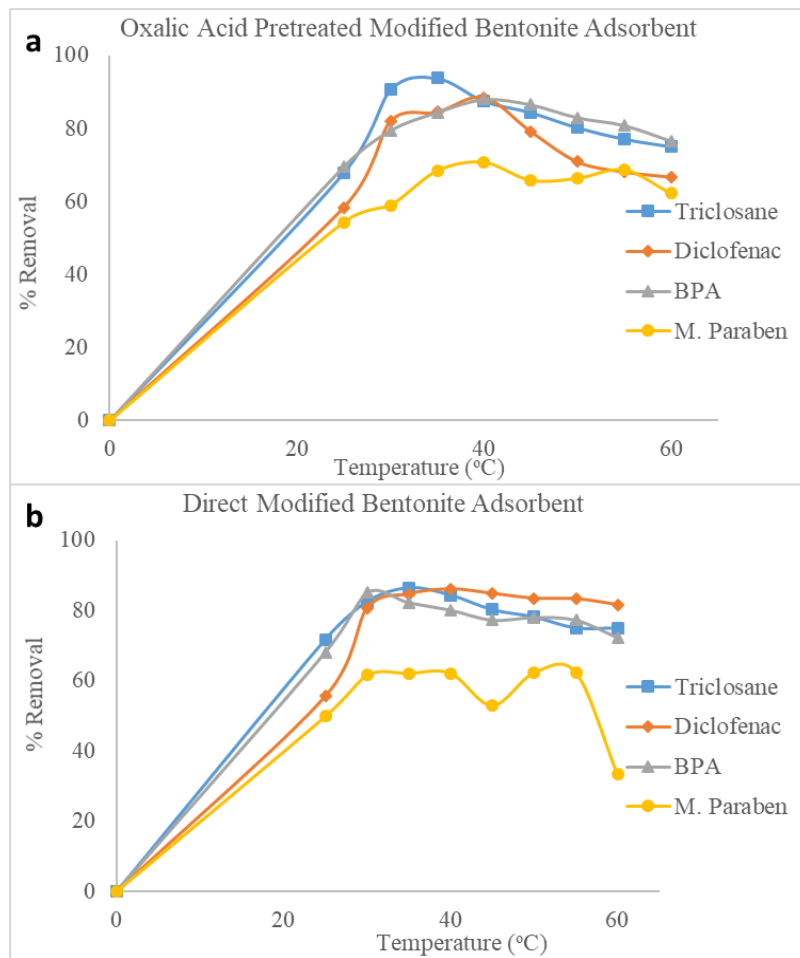
Fig. 8. Effect of temperature on ECs removal (a) Oxalic acid pretreated and (b) Direct organo-modified bentonite adsorbent

3.6 Adsorption Isotherm and Adsorption Kinetics

The study further examines adsorption isotherm and kinetics that describes the equilibrium and experimental factors that influence the adsorption rate. The results of the adsorption isotherm and kinetic are presented and discussed subsequently.

3.6.1 Adsorption isotherm

Adsorption isotherm of produced adsorbents was investigated to describes the equilibrium of the adsorption materials at the surface of adsorbent and, particularly at the surface boundary at constant temperature. The isotherm model considered in this study are Langmuir and Freundlich isotherm models which are discussed subsequently. Table 5 present the adsorption isotherm parameters of adsorbents.

The adsorption data acquired from the newly created organo-modified bentonite adsorbents were subjected to fitting using the Langmuir and Freundlich isotherm models. Table 3 presents the findings that, across all adsorbents (specifically, organo-modified bentonite adsorbents), the equilibrium of the adsorption materials at the surface of the adsorbents, and specifically at the surface boundary, is most accurately described by the Freundlich isotherm. This conclusion is supported by R^2 values within 0.9691 to 0.9984 for the Freundlich isotherm, compared to R^2 values found between 0.3899 to 0.6122 for the Langmuir isotherm. The strong agreement between the experimental data and Freundlich isotherm stated that adsorption takes place on surfaces that are heterogeneous and contain active sites. These active sites, found in both organo-modified bentonites, exhibit varying energies, indicating a process of multilayer adsorption and equilibrium [51].

Table 3. Adsorption isotherm studies

Parameters	Langmuir Isotherm				Freundlich Isotherms		
	q_{max}	b	R_L	R^2	k_f	n	R^2
Oxalic Acid Pretreated Modified Bentonite							
Triclosane	0.1074	-4.0416	-0.0114	0.5216	0.6501	3.9173	0.9984
Diclofenac	0.0291	-2.3139	-0.0202	0.5525	0.4634	1.7623	0.9850
BPA	0.0359	-0.8215	-0.0589	0.5098	0.6617	1.1626	0.9907
M. Paraben	0.0075	-0.2374	-0.2385	0.5056	2.6632	0.3293	0.9952
Direct Modified Bentonite							
Triclosane	0.0599	-0.3994	-0.1293	0.5306	1.0992	2.3077	0.9899
Diclofenac	0.0386	-0.5974	-0.0829	0.5350	0.6530	2.6111	0.9844
BPA	0.0332	-0.4513	-0.1127	0.5259	0.8372	1.9523	0.9754
M. Paraben	0.0115	-0.2664	-0.2072	0.5321	1.6111	0.9208	0.9852

Furthermore, the parameter n shows the amount and high rate of intensity of adsorption or the degree of surface heterogeneity, serves as an indicator of the energy distribution and heterogeneity of the adsorbate sites [60, 61]. From Table 3, the value of n was found to be 1.1626 – 4.2954 for both adsorbents. The value of n that was obtained in this research is above 1, indicating that all the organo-modified bentonites adsorbents are favorable for adsorption of Triclosane, Diclofenac, BPA and Methyl Paraben under conditions used in this study and further indicated that adsorption is the predominant process taking place. Furthermore, k_f which is Freundlich adsorption capacity was found to be 0.4634 – 2.6632 L/mg with the highest value of 2.6632 L/mg found for Methyl Paraben adsorption in oxalic acid pretreated modified bentonite adsorbent (Table 5). Therefore, Freundlich isotherm provides the most accurate description of the equilibrium of adsorption materials at the surface of both organo-modified bentonite adsorbents.

3.6.2 Adsorption kinetics

The investigation of the adsorption kinetics of the manufactured adsorbent aimed to explain the uptake of ECs (emerging contaminants) over time at a constant pressure. The kinetic models examined in this investigation encompass the pseudo-first order and pseudo-second-order kinetics. Table 4 present the adsorption kinetics studies of adsorbents.

The obtained adsorption kinetics data from both created organo-modified bentonite adsorbents were analyzed utilizing the pseudo-first order and pseudo-second-order kinetics models was to evaluate adsorption mechanism. Table 4 presents the adsorption behavior of Triclosane, Diclofenac, BPA, and Methyl Paraben on two types of adsorbents, namely organo-modified bentonite clay. Results generated indicated that the adsorption process for these compounds follows a pseudo-second-order kinetic model, as evidenced by high correlation coefficients (R^2 values ranging from 0.86601 to 0.99847). However, it should be noted that the adsorption of diclofenac on oxalic acid pretreated modified bentonite and BPA on direct modified bentonite deviates from this trend. In these cases, the adsorption is better described by a pseudo-first-order kinetic model, with correlation coefficients (R^2 values) ranging from 0.87891 to 0.96588.

Table 4. Adsorption kinetic studies

Parameters	First order			Second Order		
	k_1	q_e	R^2	k_2	q_e	R^2
Oxalic Acid Pretreated Modified Bentonite						
Triclosane	0.00057	20.20082	0.82280	0.00032	106.75162	0.99847
Diclofenac	0.00075	11.10395	0.92454	0.0000015	1431.21479	0.85996
BPA	0.00071	13.07059	0.86936	0.00343	39.08715	0.98818
M. Paraben	0.00037	9.09605	0.79855	0.0000048	684.68230	0.86601
Direct Modified Bentonite						
Triclosane	0.00071	20.31033	0.86294	0.00074	71.98650	0.93777
Diclofenac	0.00056	11.08101	0.90875	0.0050221	19.25855	0.97236
BPA	0.00066	13.08737	0.92310	0.00002	246.77026	0.70153
M. Paraben	0.00042	9.10216	0.91340	0.0000071	519.54807	0.93732

Adsorption of Methyl Paraben in both adsorbents exhibited the highest kinetic rate constant in the pseudo-first-order kinetic model, with values ranging from 0.00037 to 0.00054 min^{-1}. In contrast, the pseudo-second-order kinetic model yielded lower rate constants, ranging from 0.0000029 to 0.0000071 g/mg min. Furthermore, the adsorption rate constant of Triclosane in both adsorbents was determined to range from 0.00051 to 0.00071 min^{-1} for the pseudo-first-order kinetic model, and from 0.000014 to 0.00074 g/mg min for the pseudo-second-order kinetic model. In a similar vein, the adsorption rate constant of Diclofenac was determined to be within the range of 0.00034 – 0.00075 min^{-1} for the pseudo-first-order kinetic model, and 0.0000015 – 0.0061125 g/mg min for the pseudo-second-order kinetic model, in both adsorbents. Similarly, the adsorption rate constant of bisphenol A (BPA) in all adsorbents was determined to range from 0.00054 to 0.00071 min^{-1} for pseudo-first-order kinetics, and from 4.9 x 10^{-7} to 0.00343 g/mg min for pseudo-second-order kinetics. The rate constants found in this work, pertaining to both first and second-order rate constants, can be ascribed to the tendency of the adsorbate species (Triclosane, Diclofenac, BPA, and Methyl Paraben) to undergo migration from the solid phase to the bulk phase [57]. The adsorption isotherm and kinetics of Triclosane, Diclofenac, BPA, and Methyl Paraben from contaminated water were investigated using developed adsorbents. The results indicate that the equilibrium of the adsorption materials on the surface of both organo-modified bentonite clay adsorbents can be best described by the Freundlich isotherm. Additionally, the kinetics study reveals that the adsorption of Triclosane, Diclofenac, BPA, and Methyl Paraben on both adsorbents follows a pseudo-second-order kinetic model, except for diclofenac adsorption on oxalic acid pretreated modified bentonite and BPA adsorption on direct modified bentonite adsorbent.

3.6.3 Intra-particle diffusion model

Utilization of the intra-particle diffusion model was afterwards employed to assess adsorption kinetics of adsorbents. The intra-particle diffusion model offers valuable insights into the underlying mechanics for the adsorption procedure. According to this model, various mechanisms are implicated in the process of adsorption. Intra-particle diffusion can be delineated into three fundamental steps: superficial external adsorption, intra-particle diffusion as the rate-determining phase, and the subsequent attainment of equilibrium, which occurs rapidly [62, 63, 64, 65, 66]. Therefore, plot of the experimental data displays multilinear patterns which was inferred that the adsorption process was influenced by two or more processes. Fig. 9 illustrates the intraparticle diffusion model employed to describe the adsorption process of emerging contaminants (ECs) onto modified bentonite that has been prepared with oxalic acid, referred to as PMB.

Based on the observations presented in Fig. 9, it is evident that the adsorption of triclosan, diclofenac, bisphenol A (BPA), and methyl paraben (M. Paraben) onto oxalic acid PMB follows multilinear plots. This highlighted that rate-limiting step in this process is not solely governed by intra-particle diffusion. Furthermore, the negative intercept obtained for both adsorbents shows that adsorption process is intricate. Values of R^2 for the intraparticle diffusion model for the adsorption of triclosan, diclofenac, BPA, and M. Paraben into oxalic acid PMB are reported as 0.9547, 0.8651, 0.9763, and 0.9814, respectively. These values indicate a strong fit between the adsorption process and the model.

The steep initial region observed in Fig. 9 for all ECs can be linked to surface sorption. Subsequent region can be linked to intra-particle diffusion, while the final region in the plots might be as a result of equilibrium adsorption. This suggests that the adsorption process for triclosan, diclofenac, and M. Paraben follows three distinct steps. However, for BPA, the process follows two steps as indicated by the gradient not passing through the origin [67, 68]. Therefore, the adsorption rate of triclosan, diclofenac, and M. Paraben onto oxalic acid PMB was caused as a result of external or surface adsorption (film diffusion), intra-particle diffusion, and equilibrium adsorption. This is observed for triclosan, diclofenac, and M. Paraben. On the other hand, the adsorption of BPA is influenced by external or surface adsorption (film diffusion) and intra-particle diffusion.

Table 5 highlighted the rate of diffusion to be the highest at the starting point of surface sorption as it reduces in subsequent stage of region where intra-particle diffusion and equilibrium adsorption prevail. This is seen from Table 5, that $k_{id\ 1} > k_{id\ 2} > k_{id\ 3}$, in all ECs adsorbed into oxalic acid PMB. This indicates a faster sorption rate due to the availability of sufficient adsorption site at the starting point while the rate of intra-particle diffusion reduces in subsequent region as adsorption time rises. [69, 66].
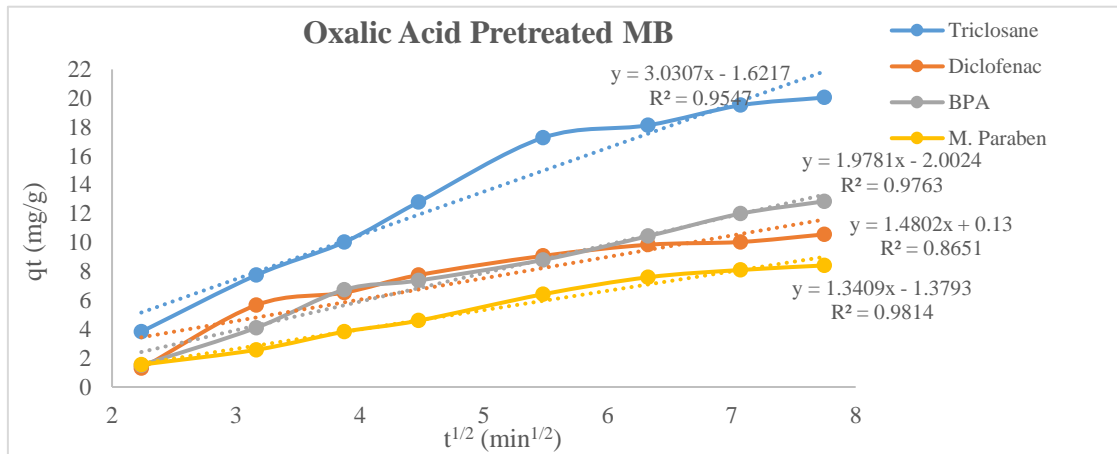
Fig. 9. Intraparticle diffusion model for the adsorption of ECs into oxalic acid pretreated MB

Table 5. Intra-particle diffusion model parameters for adsorption of ECs from wastewater

Parameters	Parameters			
	Triclosane	**Diclofenac**	**BPA**	**M. Paraben**
Oxalic Acid Pretreated Modified Bentonite				
$k_{id\,1}$, mg/g. min$^{1/2}$	3.9366	3.2784	2.7539	1.3950
$k_{id\,2}$, mg/g. min$^{1/2}$	2.9235	1.1408	1.7389	1.6283
$k_{id\,3}$, mg/g. min$^{1/2}$	1.3583	0.4988	-	0.5766
C_i	-1.6217	0.1300	-2.0024	-1.3793
k_{id}, mg/g. min$^{1/2}$	3.0307	1.4802	1.9781	1.3409
R^2	0.9547	0.8651	0.9763	0.9814
Direct Modified Bentonite				
$k_{id\,1}$, mg/g. min$^{1/2}$	4.6094	2.2260	3.2027	1.6449
$k_{id\,2}$, mg/g. min$^{1/2}$	2.1900	1.1530	1.1732	1.3366
$k_{id\,3}$, mg/g. min$^{1/2}$	1.2098	0.4409	0.5480	-
C_i	-3.5182	-0.2647	-0.8561	-1.7966
k_{id}, mg/g. min$^{1/2}$	3.0071	1.3435	1.7705	1.5237
R^2	0.9410	0.9212	0.8989	0.9855

Additionally, Fig. 10 illustrates the intraparticle diffusion model utilized in the adsorption process for triclosan, diclofenac, BPA, and M. Paraben onto direct MB (modified bentonite). The adsorption of these emerging contaminants (ECs) onto the direct MB adsorbent was characterized by a three-stage multilinear plot for triclosan, diclofenac, and BPA. In contrast, the adsorption process of M. Paraben demonstrates a two-stage multilinear plot, indicating the complexity of the adsorption process. The initial steep region observed in all electrochemical cells (ECs) can be ascribed to surface sorption. Subsequent region can be link to intra-particle diffusion. The third region observed in the plots can be attributed to equilibrium adsorption, indicating that the adsorption process for triclosan, diclofenac, and BPA follows three distinct steps. However, for M. Paraben, the adsorption process follows two steps as the

gradient does not pass through the origin. This was stated by [67, 68]. Similarly, the R2 values of the intraparticle diffusion model for the adsorption of triclosan, diclofenac, BPA, and M. Paraben onto the direct MB adsorbent are 0.9410, 0.9212, 0.8989, and 0.9855 (as presented in Table 6), respectively. These values indicate a strong fit between the adsorption process and the model.

Table 5 indicates that the rate of diffusion is highest at the beginning of surface sorption while it reduces in subsequent stage of region where intra-particle diffusion and equilibrium adsorption prevail which is seen from $k_{id\,1} > k_{id\,2} > k_{id\,3}$ in all ECs adsorbed into direct MB. This indicates a faster sorption rate at the starting point while the rate of intra-particle diffusion reduces in subsequent region as adsorption time increases. This behavior can be link to high-rate adsorption

capacity which was recorded at initial stage of the adsorption process [69, 66]. Hence, the adsorption rate of triclosan, diclofenac, and BPA onto the direct MB adsorbent is affected by surface adsorption, intra-particle diffusion, and equilibrium adsorption. Conversely, the adsorption of M Paraben onto direct MB is determined solely by surface adsorption and intra-particle diffusion.

3.7 Adsorption Activation Energy

Studies on the activation energy of adsorption procedure was conducted using the Arrhenius equation to evaluate the chemical interaction

between the contaminants and the adsorbent. The determination of activation energy (Ea) is of utmost importance in the field of adsorption research which provides valuable insights into the underlying mechanisms of adsorption. Activation energy (Ea) values for physical adsorption typically fall between 5 - 40 kJ/mol. In contrast, chemisorption, which involves the creation of strong bonding which necessitates an energy interval of 40 – 800 kJ/mol [70, 63, 64, 65, 71]. Table 7 displays the activation energy values pertaining to the adsorption process of triclosan, diclofenac, BPA, and M. Paraben onto the two modified bentonite adsorbents.

Table 6. Intra-particle diffusion model parameters for adsorption of ECs from wastewater

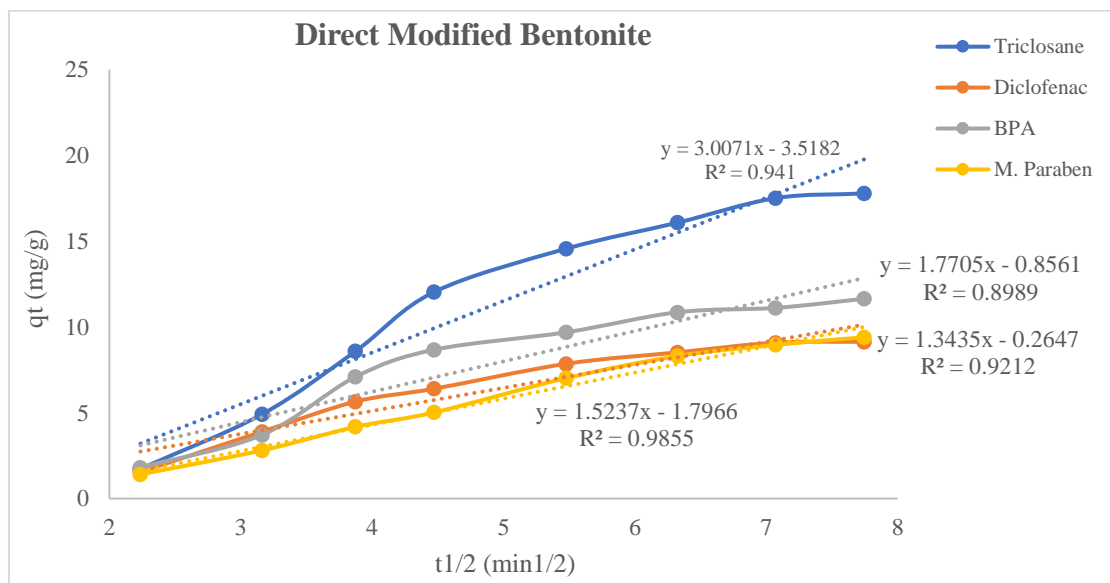| Parameters	Parameters			
Parameters	Triclosane	Diclofenac	BPA	M. Paraben
Oxalic Acid Pretreated Modified Bentonite				
$k_{id\,1}$, mg/g. min$^{1/2}$	3.9366	3.2784	2.7539	1.3950
$k_{id\,2}$, mg/g. min$^{1/2}$	2.9235	1.1408	1.7389	1.6283
$k_{id\,3}$, mg/g. min$^{1/2}$	1.3583	0.4988	-	0.5766
Ci	-1.6217	0.1300	-2.0024	-1.3793
k_{id}, mg/g. min$^{1/2}$	3.0307	1.4802	1.9781	1.3409
R^2	0.9547	0.8651	0.9763	0.9814
Direct Modified Bentonite				
$k_{id\,1}$, mg/g. min$^{1/2}$	4.6094	2.2260	3.2027	1.6449
$k_{id\,2}$, mg/g. min$^{1/2}$	2.1900	1.1530	1.1732	1.3366
$k_{id\,3}$, mg/g. min$^{1/2}$	1.2098	0.4409	0.5480	-
Ci	-3.5182	-0.2647	-0.8561	-1.7966
k_{id}, mg/g. min$^{1/2}$	3.0071	1.3435	1.7705	1.5237
R^2	0.9410	0.9212	0.8989	0.9855

Fig. 10. Intraparticle diffusion model for the adsorption of ECs into direct MB

Table 7. Adsorption activation energy

Parameters	E_a (kJ/mol)	k_o (g/mg.min)
Oxalic Acid Pretreated Modified Bentonite		
Triclosane	12.074	3.549
Diclofenac	9.820	0.007
BPA	10.665	20.499
M. Paraben	10.204	0.016
Direct Modified Bentonite		
Triclosane	9.952	3.483
Diclofenac	11.751	45.652
BPA	13.876	0.374
M. Paraben	8.952	0.013

From Table 7, the Ea energy for the adsorption of all ECs (triclosan, diclofenac, BPA and M. Paraben) into oxalic acid PMB is in the range of 9.80 – 12.10 kJ/mol, 8.90 – 13.90 kJ/mol for direct MB adsorbents. This indicates that the adsorption mechanism of triclosan, diclofenac, BPA and M. Paraben into oxalic acid PMB and the direct MB adsorbent were within energy range of 5 – 40 kJ/mol for physio-sorption [69, 72, 64, 65, 70]. The Ea value less than 40 kJ/mol for both adsorbents suggest that there is no chemical interaction in adsorption process for all adsorbents and that lesser energy of activation is required for the adsorption of all ECs into the adsorbents which implies that equilibrium will be reach in lesser adsorption time. Hence, the adsorption mechanism of triclosan, diclofenac, BPA and M. Paraben into oxalic acid PMB and the direct MB adsorbents is physio-sorption and diffusion-controlled.

4. CONCLUSION

Emerging contaminants (ECs) are a diverse group of anthropogenic substances that have been found to be harmful to all living things. They are estimated to have increased from the range of one million to five hundred million tons every year and are essential to modern society worldwide. Environmental scientists worldwide are focusing their research on improving the re-use of treated wastewater by identifying and developing technological treatment methods and filling knowledge gaps on the elimination of ECs in water. This study compared removal efficiency of ECs present in wastewater using adsorbents made of organo-modified bentonite clay. From the study carried out, the following conclusions are made; The major ECs identified using HPLC from wastewater are mainly Diclofenac, Triclosan, Methylparaben, and Bisphenol A which are detrimental to human health and environments, and the adsorption and kinetics studies focuses on the identified ECs (Diclofenac, Triclosan, Methylparaben and Bisphenol A) with the highest concentration which account for 76.206% of the ECs in the wastewater. organo-modified bentonite clay adsorbents were successfully produced from bentonite clay with two separate samples of bentonite clay adsorbent produced (oxalic acid pretreated modified bentonite clay adsorbent and untreated modified bentonite clay adsorbent). The produced acid-pretreated organo-modified bentonite adsorbents possess higher adsorption capacity for ECs removal from wastewater. Also, the adsorbent characterization shows that the morphology of the produced acid-pretreated organo-modified bentonite adsorbents has better pore development with a higher amorphous structure that enhances the uptake of contamination into the adsorbents. acid-pretreated modified bentonite adsorbent shows the highest removal rate for Triclosane, Diclofenac, and BPA compared to direct modified bentonite clay. Also, acid-pretreated modified bentonite adsorbent shows the highest removal rate for Triclosane, Diclofenac, and BPA at 2 – 2.5 g adsorbent dosage with the lowest Methyl-Paraben removal rate when compared to the other direct modified adsorbent. On the other hand, growing efficacy has also been shown in the synthesis of new clay-based solids with specialized characteristics for the uptake of certain chemicals and this was also reported by the following studies [73,74,75]. While at higher temperatures, the molecule of the ECs gets lighter and can move freely and fast out of the pores of the adsorbent thereby resulting in an increased rate of desorption of the ECs back into the bulk solution as observed during the study [56]. The decrease in the rate of adsorption by both adsorbents with increasing temperature signifies a low energy requirement for ECs adsorption onto oxalic acid pretreated organo-

modified bentonite and direct organo-modified bentonite adsorbent.

From the adsorption isotherm and kinetics study of Triclosane, Diclofenac, BPA, and Methyl Paraben from contaminated water by both developed adsorbents, the Freundlich isotherm best described the equilibrium of the adsorption properties at the surface of both organo-modified bentonites while the kinetics study shows that Triclosane, Diclofenac, BPA and Methyl Paraben adsorption in both adsorbents favors pseudo-second-order kinetic model; except diclofenac adsorption in oxalic acid pretreated modified bentonite; BPA adsorption in direct modified bentonite; Triclosane.

Finally, intraparticle diffusion model shows rate of adsorption of ECs into both adsorbents which was influenced by surface adsorption, intra-particle diffusion, and equilibrium adsorption or by surface adsorption and intra-particle diffusion alone while adsorption mechanism of triclosan, diclofenac, BPA, and M. Paraben into oxalic acid PMB and the direct MB adsorbents was physio-sorption and diffusion-controlled.

ACKNOWLEDGEMENT

COMPETING INTERESTS

Authors have declared that no competing interests exist.

REFERNCES

1. UNDP. Report on the human development. United Nations Development Program beyond the Shortage: power, Poverty and the World Crisis of the Water, New York; 2006.

2. Olaniyi OT. Surfactant-Modified Adsorbents for the Removal of Toxic Anions in Water. MSc Thesis in Environmental and Analytical Chemistry, Redeemer's University, Ede, Osun State: 15; 2016.

3. Rasheed T, Bilal M, Nabeel F, Adeel M, Iqbal HMN. Environmentally related contaminants of high concern: potential sources and analytical modalities for detection, quantification, and treatment. Environ Int. 2019;122:52-66.
DOI: 10.1016/j.envint.2018.11.038, PMID 30503315.

4. Lellis B, Fávaro-Polonio CZ, Pamphile JA, Polonio JC. Effects of textile dyes on health and the environment and bioremediation potential of living organisms. Biotechnol Res Innov. 2019;3(2):275-90.

5. Bilal M, Asgher M, Parra-Saldivar RP, Hu H, Wang W, Zhang X et al. Immobilized ligninolytic enzymes: an innovative and environmental responsive technology to tackle dye-based industrial pollutants–a review. Sci Total Environ. 2017;576:646-59.

6. Liu L, Wang L, Song W, Yang L, Yin L, Xia S et al. Crude oil removal from aqueous solution using raw and carbonized Xanthoceras sorbifolia shells. Environ Sci Pollut Res Int. 2018;25(29):29325-34.
DOI: 10.1007/s11356-018-2895-0, PMID 30121766.

7. Zhang Y, Yan L, Xu W, Guo X, Cui L, Gao L et al. Adsorption of Pb(II) and Hg(II) from aqueous solution using magnetic CoFe2O4-reduced grapheme oxide. J Mol Liq. 2014;191:177-82.

8. Osin OA, Yu TY, Lin SJ. Oil refinery wastewater treatment in the Niger Delta, Nigeria: current practices, challenges, and recommendations. Environ Sci Pollut Res Int. 2017;24(28):22730-40.
DOI: 10.1007/s11356-017-0009-z

9. Lv N, Wang X, Peng S, Zhang H, Luo L. Study of the kinetics and equilibrium of the adsorption of oils onto hydrophobic jute fiber modified via the sol-gel method. Int J Environ Res Public Health. 2018;15(5):1-14.
DOI: 10.3390/ijerph15050969

10. Mokif LA. Removal methods of synthetic dyes from industrial wastewater: a review. Mesop Environ J. 2019;5.

11. Vijayageetha V, Rajan AP, Arockiaraj S, Annamalai V, Janakarajan V, Balaji MS et al. Res. J Recent Sci. 2014;3:58-61.

12. Huang R, Zhang QI, Yao H, Lu X, Zhou Q, Yan D. Ion -exchange resins for efficient removal of colorants in bis (hydroxyethyl)terephthalate. ACS Omega. 2021;6(18):12351-60.

13. Torkian N, Bahrami A, Hosseini-Abari A, Momeni MM, Abdolkarimi-Mahabadi M, Bayat A et al. Synthesis and characterization of Ag-ion exchanged zeolite/TiO2 nanocomposites for antibacterial applications and photocatalytic degradation of antibiotics. Environ Res. 2022;207:Article 112157.

14. Chanikya P, Nidheesh P, Badu DS, Gopinath A, Kumar MS. Treatment of dyeing by combined sulfate radical based electrochemical advanced oxidation and electrocoagulation processes. Sep Purif Technol. 2021;254:Article 117570.

15. Alwan SH, Alshamsi HA. In situ synthesis NiO/F-MWCNTs nanocomposite for adsorption of malachite green dye from polluted water. Carbon Lett. 2022;32(4):1073-84.

16. Powar AS, Perwuelz A, Behary N, Hoang L, Aussenac T. Application of ozone treatment for the decolorization of the reactive- dyed fabrics in a pilot -scale process- optimization through response surface methodology. Sustainability. 2020;12(2):471.

17. Ajel MK, Al-Nayili A. Synthesis, characterization of Ag -WO3/bentonite nanocomposites and their application in photocatalytic degradation of humic acid in water. Environ Sci Pollut Res Int. 2023;30(8):20775-89.

18. Foroutan R, Zareipour R, Mohammadi R. Fast adsorption of chromium (VI) ions from synthetic sewage using bentonite and bentonite/biocoal composite: A comparative study. Mater Res Express. 2018;1-26.

19. Ahmed MB, Zhou JL, Ngo HH, Guo W. Adsorptive removal of antibiotics from water and wastewater: progress and challenges. Sci Total Environ. 2015;532:112-26.

20. Alhassan M, Andrew I, Auta M, Umaru M, Garba UG, Isah AG et al. Comparative studies of CO_2 capture using acid and base modified activated carbon from sugarcane bagasse. Biofuels; 2017. DOI:10.1080/17597269.2017.1306680

21. Uddin MK. A review on the adsorption of heavy metals by clay minerals, with special focus on the past decade. Chem Eng J. 2017;308:438-62.

22. Momina M, Mohammad S, Suzylawati I. A review on Regeneration performance of clay-based adsorbents for the removal of industrial dyes. J R Soc Chem. 2018:24571-87.

23. Sheeja J, Sampath K, Kesavasamy R, Sen T. Experimental investigations on adsorption of reactive toxic dyes using Hedyotis umbellate activated carbon. Adsorpt Sci Technol. 2021;2021:1-12.

24. Hammood ZA, Chyad TF, Al-Saedi R. Adsorption performance of dyes over zeolite for textile wastewater treatment. Ecol Chem Eng S. 2021;28(3):329-37.

25. Martinez Stagnaro SY, Volzone C. Adsorption of anionic dyes monoazo and diazo using organo bentonites. SN Appl Sci. 2019;1(1):70.

26. El-Bery HM, Saleh M, El-Gendy RA, Saleh MR, Thabet SM. High adsorption capacity of phenol and methylene blue using activated carbon derived from lignocellulosic agriculture wastes. Sci Rep. 2022;12(1):5499.

27. Ibrahim SM, Hassanin HM, Abdelrazek MM. Synthesis, and characterization of chitosan bearing pyranoquinolinone moiety for textile dye adsorption from wastewater. Water Sci Technol. 2020;81(3):421-35.

28. Yahia M, Youssef HF, Elfeky AS, Award M-B-E-D, Elzaref A. Induced effects of gamma irradiation on activated carbon derived from Hyphaene thebaica husks as a potential adsorbent for chlorpyrifos pesticide- air purification. Egypt J Chem. 2022;65:449-74.

29. Mok CF, Ching YC, Muhamad F, Abu Osman NA, Hai ND, Che Hassan CR. Adsorption of dyes using poly (vinyl alcohol) (PVA) and PVA- based polymer composite adsorbents: a review. J Polym Environ. 2020;28(3):775-93.

30. Kar P, Jain P, Gupta RK, Tripathi KM. Emerging carbon -based nanocomposites for remediation of heavy metals and organic pollutants from wastewater. A.K. Mishra, C.M. Hussain, S.B Mishra (Eds), Emerging carbon-based nanocomposites for Environmental Applications, Willey. 2020;1-29.

31. Paton-Carrero A, Sanchez P, Sánchez-Silva L, Romero A. Graphene-based materials behaviour for dyes adsorption. Mater Today Commun. 2022;30:Article 103033.

32. Rasheed T, Li C, Bilal M, Yu C, Iqbal HMN. Potentially toxic elements and environmentally related pollutants recognition using colorimetric and

ratiometric fluorescent probes. Sci Total Environ. 2018;640-641:174-93.

33. El-Zahhar AA, Al-Hazmi GA. Organically modified clay for adsorption of petroleum hydrocarbon. Eur Chem Bull. 2015;4(2):87-91.

34. Albo Hay Allah MA, Alshamsi HA. Green synthesis of AC/ZnO nanocomposites for adsorptive removal of organic dyes from aqueous solution. Inorg Chem Commun. 2023;157:111415.
DOI: 10.1016/j.inoche.2023.111415.

35. Albo Hay Allah MA, Alshamsi HA. Facile green synthesis of ZnO/AC nanocomposites using Pontederia crassipes leaf extract and their photocatalytic properties based on visible light activation. J Mater Sci Mater Electron. 2023;34(16):1263.
DOI: 10.1007/s10854-023-10636-y.

36. Mandal S, Kunhikrishnan A, Naidu R. Development in Aquaculture and Fisheries Science. Chapter 4: Application of Biochar Produced from Biowaste Materials for Environmental Protection and Sustainable Agriculture Production. Environmental Materials and Waste. 2016;73 – 89.

37. Corcoll N, Acuña V, Barceló D, Casellas M, Guasch H, Huerta B et al. Pollution-induced community tolerance to non-steroidal anti-inflammatory drugs (NSAIDs) in fluvial biofilm communities affected by WWTP effluents. Chemosphere. 2014;112:185-93.

38. De-Coster S, Van-Larebeke N. Endocrine Disrupting Chemicals: Associated Disorders and Mechanism of Acion. Journal of Environment and Public Health. Hindawi Publishing Corporation. 2012;2012(Article ID):713696:1 – 50.

39. Gomes IB, Simões LC, Simões M. The effects of emerging environmental contaminants on Stenotrophomonas maltophilia isolated from drinking water in planktonic and sessile states. Sci Total Environ. 2018;643:1348-56.

40. Ilnegbenebor AI, Sanya OOP, Ogunniran KO, Negbenebor A. Potentially Exploitable Base-Metal Containing Bentonite Clay Minerals of Ibeshi-Ikorodu South-Western Nigeria for Oil Bleaching, Covenant Journal of Physical and Life Sciences (CJPL). 2014;2(2):123 – 125.

41. Parolo ME, Pettinari GR, Musso TB, Sánchez-Izquierdo MP, Fernández LG. Characterization of organo-modified bentonite sorbents: the effect of modification conditions on adsorption performance. Appl Surf Sci. 2014;320:356-63.

42. Zhang L, Yuan H, Meng Y, Mao H. Development of high-pressure multigrain X-ray diffraction for exploring the earth's interior. Engineering. 2019;5(3):441-7.
DOI: 10.1016/j.eng.2019.02.004.

43. Ammar M, Oueslati W, Ben Rhaiem H, Ben Haj Amara A. Effect of the hydration sequence orientation on the structural properties of Hg exchanged montmorillonite: quantitative XRD analysis. J Environ Chem Eng. 2014;2(3):1604-11.
DOI: 10.1016/j.jece.2014.05.022.

44. Timofeeva MN, Panchenko VN, Krupskaya VV, Gil A, Vicente MA. Effect of nitric acid modification of montmorillonite clay on synthesis of solketal from glycerol and acetone. Cat Commun. 2017;90:65-9.
DOI: 10.1016/j.catcom.2016.11.020.

45. Milinovic J, Dias ÁA, Janeiro AI, Pereira MFC, Martins S, Petersen S et al. XRD identification of ore minerals during cruises: refinement of extraction procedure with sodium acetate buffer. Minerals. 2020;10(2):160.
DOI: 10.3390/min10020160.

46. Borisov SV, Magarill SA, Pervukhina NV. Crystallographic analysis of the garnet structure type: symmetry in the structural anatomy. J Struct Chem. 2018;59(2):365-70.
DIO:10.1134/S0022476618020154.

47. Adeyemo AA, Adeoye IO, Bello OS. Adsorption of dyes using different types of clay: a review. Appl Water Sci. 2015:1-26.
DOI: 10.1007/s13201-015-0322-y.

48. Sierra-Fernandez A, Gomez-Villalba LS, Milosevic O, Fort R, Rabanal MESynthesis and morpho-structural characterization of nanostructured magnesium hydroxide obtained by a hydrothermal method. Ceram Int. 2014;40(8):12285-92.
DOI: 10.1016/j.ceramint.2014.04.073.

49. Zuena M, Tomasin P, Costa D, Delgado-Rodrigues J, Zendri E. Study of calcium ethoxide as a new product for conservation of historical limestone. Coatings. 2018;8(3):103.
DOI: 10.3390/coatings8030103.

50. Abdullahi S, Audu AA. Comparative analysis on chemical composition of bentonite clays obtained from Ashaka and tango deposits in Gombe State, Nigeria. ChemSearch Journal. 2017;8:35-40.

51. Afolabi RO, Orodu OD, Efeovbokhan VE. Properties and application of Nigerian bentonite clay deposits for drilling mud formulation: recent advances and future prospects. Appl Clay Sci. 2017;143:39-49.

52. Ravisankar RR, Senthilkumar G, Kiruba S, Chandrasekaran A, Jebakumar PP. Mineral analysis of coastal sediment samples of Tuna, Gujarat, India. Indian J Sci Technol. 2010;3(7):774-80.

53. Wang S, Gao B, Li Y, Mosa A, Zimmerman AR, Ma LQ et al. Manganese oxide-modified biochars: preparation, characterization, and sorption of arsenate and lead. Bioresour Technol. 2015;181:13-7.

54. Rahimi-Nasrabadi M, Behpour M, Sobhani-Nasab A, Mostafa Hosseinpour-Mashkani S. $ZnFe_{2-x}La_xO_4$ nanostructure: synthesis, characterization, and its magnetic properties. J Mater Sci Mater Electron. 2015;26(12):9776-81.
DOI: 10.1007/s10854-015-3648-1.

55. Ramírez-Ortega D, Acevedo-Peña P, Tzompantzi F, Arroyo R, González F, González I. Energetic states in SnO 2–TiO 2 structures and their impact on interfacial charge transfer process. J Mater Sci. 2017;52(1):260-75.
DOI: 10.1007/s10853-016-0328-3.

56. Hokkanen S, Bhatnagar A, Srivastava V, Suorsa V, Sillanpää M. Removal of Cd^{2+}, Ni^{2+} and PO_4^{3-} from aqueous solution by hydroxyapatite-bentonite claynanocellulose composite. Int J Biol Macromol. 2018;118(A):903-12.

57. Edet UA, Ifelebuegu AO. Kinetics, isotherms, and thermodynamic modeling of the adsorption of phosphates from model wastewater using recycled brick waste. Processes. 2020;8(6):1-15.
DOI: 10.3390/pr8060665.

58. Emam EA. Modified activated carbon and bentonite used to adsorb petroleum hydrocarbons emulsified in aqueous solution. Am J Environ Prot. 2013;2(6):161-9.

59. Gandhi N, Sirisha D, Sekhar KC. Adsorption of chromium (VI) from aqueous solution by using Multani Miti. Int J Res Pharm Chem. 2014;4(1):168-80.

60. Okoli IZ. Adsorption studies of heavy metals by low-cost adsorbents. J Appl Sci Environ Manag. 2014;18(3):443-8.

61. Ayawei N, Ebelegi AN, Wankasi D. Modelling and interpretation of adsorption isotherms. J Chem. 2017;2017:1-11:Article ID 3039817.
DOI: 10.1155/2017/3039817.

62. Rashidi NA, Yusup S, Lam HL. Kinetic studies on CO2 capture using activated carbon. Chem Eng Trans. 2013;35: 361-6.

63. Abdulsalam A, Mohammed A, Abubakar GI, Kovo AS, Olanrewaju A. Olalekan. Comparative Studies on The Kinetics of Biogas Purification Using Activated Carbon and Zeolite, IOP Conference Series: Earth and Environmental Science. 2018; 173(012046):1 – 13.

64. Abdullahi A, Mohammed A. Studies on biogas purification using activated carbon and zeolite. LAP Lambert academic publishing; 2018. ISBN: 978-613-9-92398-4.

65. Alhassan M, Andrew I, Auta M, Umaru M, Garba UG, Isah AG et al. Comparative studies of CO2 capture using acid and base modified activated carbon from sugarcane bagasse. Biofuels; 2017.
DOI: 10.1080/17597269.2017.1306680.

66. Romero JR, Piraján JC, Gutierrez L. Kinetic and equilibrium study of the adsorption of CO2 in ultramicropores of resorcinol-formaldehyde aerogels obtained in acidic and basic medium. C. 2018;4(4):52.

67. Nethaji S, Sivasamy A, Mandal AB. Adsorption isotherms, kinetics and mechanism for the adsorption of cationic and anionic dyes onto carbonaceous particles prepared from Juglans regia shell biomass. Int J Environ Sci Technol. 2013;10(2):231-42.

68. Kajjumba GW, Emik S, Öngen A, Özcan HK, Aydın S. Modelling of adsorption kinetic processes—errors, theory and application. In: Advanced sorption process applications. IntechOpen; 2018.
DOI: 10.5772/intechopen.80495.

69. Yan LG, Qin LL, Yu HQ, Li S, Shan RR, Du B. Adsorption of acid dyes from aqueous solution by CTMAB modified bentonite: kinetic and isotherm modeling. J Mol Liq. 2015;211:1074-81.

70. Randhawa NS, Gharami K, Kumar M. Leaching kinetics of spent nickel-cadmium battery in sulphuric acid. Hydrometallurgy. 2016;165:191-8.

71. Biswas RH, Herman F, King GE, Braun J. Thermoluminescence of feldspar as a multi-thermochronometer to constrain the

temporal variation of rock exhumation in the recent past. Earth Planet Sci Lett. 2018;495:56-68.
DOI: 10.1016/j.epsl.2018.04.030.

72. Abdullahi A, Alhassan M, Isah AG, Sani KA, Olalekan OA. Comparative studies on the kinetics of biogas purification using activated carbon and zeolite. IOP Conf S Earth Environ Sci. 2018;173 (1).
DOI: 10.1088/1755-1315/173/1/012046.

73. Khan S, Ajmal S, Hussain T, Rahman MU. Clay-based materials for enhanced water treatment: adsorption mechanisms, challenges, and future directions. JUmm Al-Qura Univ Appll Sci. 2023.
DOI: 10.1007/s43994-023-00083-0.

74. Almeida-Naranjo CE, Guerrero VH, Villamar-Ayala CA. Emerging contaminants and their removal from aqueous media using conventional/nonconventional adsorbents: A glance at the relationship between materials, processes, and technologies. Water. 2023;15(8):1626.
DOI: 10.3390/w15081626.

75. De Farias MB, Spaolonzi MP, Da Silva TL, Da Silva MGC, Vieira MGA. Natural and synthetic clay-based materials applied for the removal of emerging pollutants from aqueous medium. Adv Mater Sustain Environ Rem. 2022:359-92.
DOI: 10.1016/B978-0-323-90485-8.00012-6.

Peer-review history:
The peer review history for this paper can be accessed here:
https://www.sdiarticle5.com/review-history/108445